ACCURACY AND ADVANTAGES OF HYBRID SOLUTIONS COMPARED TO DIRECT NOISE CALCULATIONS FOR LOW-SPEED FAN NOISE

Korcan KUCUKCOSKUN[1], Axel KIERKEGAARD[2]

[1] Siemens Digital Industries Software, Simulation and Test Solutions, Interleuvenlaan 68. B-3001, Leuven, Belgium

[2] Siemens Digital Industries Software, Simulation and Test Solutions, Otto-Hahn-Ring 6. 81739 Munich, Germany

SUMMARY

Alternative acoustic simulation techniques are applied to a low-speed axial fan noise problem. Both a reference Direct Noise Calculation (DNC) solution and several hybrid propagation methods available in literature are considered. The propagation methods in time and frequency domains are compared using incompressible and compressible flow output. They are cross-validated with the DNC. Once validated in free-field, the extra benefits of the hybrid methods are demonstrated. It is shown that, without recomputing the flow solution, the hybrid techniques also enable engineers to perform contribution analysis of noise sources on fan blade segments and to include reflection and absorption effects of the industrial fans in actual installation.

INTRODUCTION

In most industrial applications it is widely accepted that noise is a concern for fan manufacturers due to comfort trends and regulations. However, fan noise prediction is not a headache for engineers anymore thanks to semi-analytical methods [1, 2] and more advanced and mature numerical simulation techniques [3, 4] backed up by increasingly available computational resources. Additionally, for most of the low-speed fan noise problems, the flow field can be separated from the acoustic field, enabling so-called hybrid methodologies.

Engineers need to select which is the more suitable approach for their applications at hand. Multiple alternative numerical techniques will give the same acoustic response for simple setups, like in a free-field radiation. However, their results may differ in more challenging setups involving for instance also the acoustic influence of the environment in which they are inserted. Based on their needs, engineers can still choose methods such as:

- A Direct Noise Calculation (DNC) from a compressible Computational Fluid Dynamics (CFD) solution as a reference solution
- A hybrid solution where the compressible flow results are coupled with a time domain acoustic propagation technique
- A hybrid solution where the incompressible flow results are coupled with a time domain acoustic propagation technique
- A hybrid solution where the compressible flow results are coupled with a frequency domain acoustic propagation technique
- A hybrid solution where the incompressible flow results are coupled with a frequency domain acoustic propagation technique

and other non-listed methods. All five alternative techniques listed above are applied to a small low-speed axial fan with acoustically compact blades for the frequencies of interest.

First, the accuracy of the hybrid solutions is challenged in a free-field radiation setup, to demonstrate that all five simulation approaches converge to the same acoustic levels in an anechoic-room like environment. Both tones and broadband responses are cross-validated using a finite-volume solution in one hand, and a finite element model on the other hand.

Later, the hybrid solution is applied to the free-field solution once more, in order to perform a contribution analysis between two zones representative of the leading-edge and trailing-edge of the blades. This demonstrates how further acoustic insight can be obtained on source locations without re-running the flow solution and how a hybrid solution complements the workflow.

Finally, the acoustic response of an installed fan is computed using the same flow results around the axial fan. The reflection and scattering due to surrounding surfaces are then considered in the finite element acoustic solution. This shows how a frequency domain acoustic solution complements a time domain finite volume flow solution in presence of installation effects in the propagation domain.

FLOW FIELD SOLUTION

A simplified virtual low-speed five-blade axial fan in free-field is considered. Rectangular blade profiles are chosen with rounded edges over both leading-edge, trailing-edge and tip regions. The hub and tip radii are selected as 0.01 m and 0.04 m, respectively. The rotation speed is selected as 6000 RPM corresponding to a Blade Passing Frequency (BPF) equal to 500 Hz.

The flow simulations are computed with two transient setups, one with incompressible and another with compressible. A spherical solution domain is chosen which also includes microphones located 10 tip radii away from the rotation center in various angles. The microphones are kept in the fluid domain in order to provide the reference DNC solution without using any acoustic analogy. The flow simulation is performed with the commercial software Simcenter STAR-CCM+ [5]. Improved Delayed Detached Eddy Simulation (IDDES) is used with Spalart-Allmaras turbulence model with 18 Million polyhedral cells. The time step is selected as 2E-5 seconds. For the compressible flow solution, non-reflecting treatment is applied on the boundaries of the fluid region.

An additional jet stream is introduced to trigger extra noise sources and to amplify radiated free-field noise levels. The jet is positioned one fan diameter upstream and off the fan's rotation axis, to introduce a non-uniform flow distribution impinging on blade leading edge locally. The jet is realized as a time independent volume source term added in the momentum equation which is implemented as a user defined field function in Simcenter STAR-CCM+. This source term accelerates the flow locally without introducing any geometric entry which could cause acoustic scattering. The fan geometry and the impinging jet can be seen in Figure 1 together with the λ_2 vortex criterion plots. The flow is from left to right and rotation is in clockwise direction.

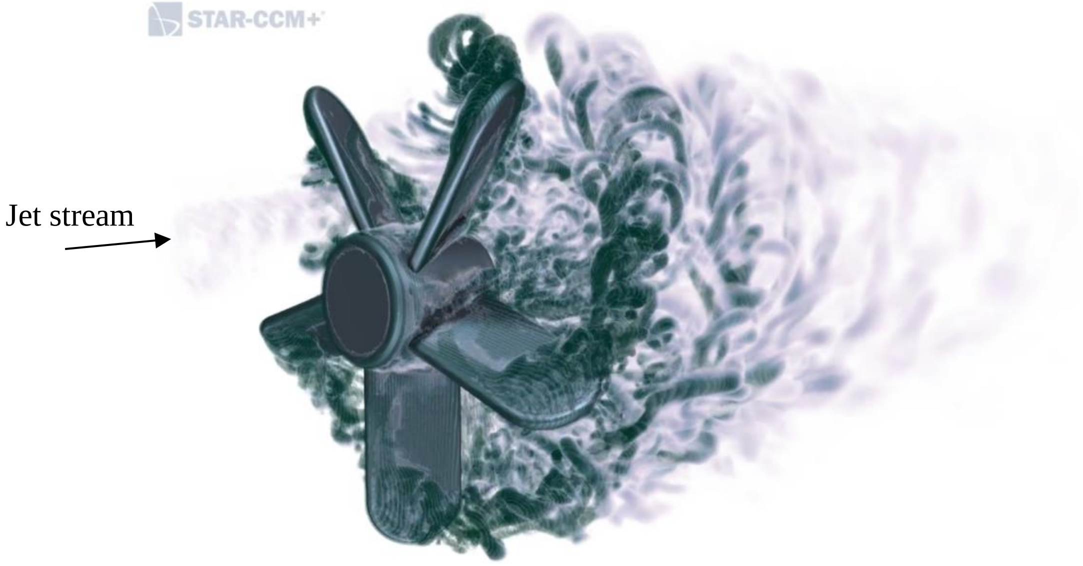

Figure 1: Fan geometry under impinging jet and λ_2 vortex criterion plots

ACOUSTIC SIMULATION METHODOLOGIES

As mentioned above, the first acoustics simulation alternative is selected as DNC, where the microphones are located in the compressible flow domain. In this method, the microphones record the total pressure signal which includes both aerodynamic and aeroacoustic components. In order to separate the acoustic results, more sophisticated post-processing methods need to be applied to the recorded pressure values, which is not addressed in this paper.

In such low-speed fan applications, one can assume that the acoustic field does not affect the flow field. Therefore, the acoustic field can be decoupled from the flow solution. A sequential hybrid simulation can then be applied to such problems; a flow field solution followed by an acoustic propagation. The Ffowcs Williams-Hawkings (FW-H) analogy [6] is widely used for such hybrid aeroacoustics application which includes rotating sources. In theory, this analogy can be used for all three components of the fan noise: Loading, thickness, and volume sources. For the considered low-speed fan application, the thickness and volume sources are assumed to be negligible, reducing to the noise sources only on the pressure loading on fan blades. Therefore, the loading noise source is assumed to be the dominant noise source. This assumption will be considered for the rest of the analogies presented in this paper.

The first alternative method to DNC addressed is using an FW-H analogy implementation in time domain [7]. Since only the loading noise is considered, the source domain is reduced to the rigid, hence impermeable, blade surfaces. This analogy computes the propagation of the acoustic waves in a retarded time approach using free-field propagation assumption. Since this analogy is independent from the density fluctuations at the source surface, and as long as the blade surfaces are considered acoustically compact, it can be used for incompressible and compressible flow simulations. Both of them are considered in this paper as separate alternatives to approach to the fan noise problem. Commercial software Simcenter STAR-CCM+ [5] is used to compute the time domain acoustic propagation to far-field observers. The compressible finite volume simulation was directly evaluated at the far-field observers of the DNC simulation where the hybrid acoustic analysis was applied on top. This approach seamlessly provides the acoustic results in free-field without extra data transfer or changing environment.

Another set of alternative hybrid solutions is to compute the propagation in frequency domain. This might simplify the propagation simulation by avoiding retarded time concerns and also letting to consider the installation effects due to complex reflective geometries and absorbing surfaces which cannot be assumed as free-field anymore.

For frequency domain propagation, one can use the incident-scattered field formulas available in literature [8, 9] where the rotation is represented analytically. This formulation would be limited to the homogenous domain due the selection of Green's function. For some industrial applications, propagation within non-homogenous domains such as porous components, or even convection effects of acoustic field due background non-uniform mean flow might be needed. Therefore, instead of an incident-scattered field approach, a so-called Right-Hand Side (RHS) implementation will be more useful for industrial applications to account for non-homogenous propagation domain and convection effects. Since only the loading noise is considered, this can be achieved by using dipole sources in the fan blade trajectory. The dipole source strength is obtained by integrating the transient pressure field over the compact blade segment.

The frequency domain Helmholtz solver used in the fan noise problem is based on Finite Element Method Adaptive Order (FEMAO) [10]. The rotating transient source terms are first projected to high-order degrees-of-freedom of the finite element problem during their trajectory which is later converted to the frequency domain via a Fourier Transform. The FEMAO problem is then solved with the RHS fan source together with proper non-reflective boundary conditions. Such non-reflective conditions are defined with Automatically Matched Layer (AML) boundaries on the envelope of the acoustic finite element domain [11].

Commercial software Simcenter 3D [12] is used for the solution of the hybrid fan noise problem in frequency domain yet using the transient blade pressure data exported from the CFD simulations described above as input. Both compressible and incompressible CFD output are used in noise source generation as two alternative solutions. This hybrid method is beneficial to take the reflective and absorbing surfaces into account. Also, without re-computing the CFD solution, one can perform contribution analysis of the dominant noise source areas propagated by the fan blade segments.

RESULTS

The flow field around the fan described above is first simulated in a free-field like CFD domain with the impinging jet using both compressible and incompressible formulations over the same domain. In order to obtain converged statistics for this study, overall, 65 rotations of the fan are considered. Please note that such a high number of rotations is not needed for industrial applications in practice.

The microphone pressure results are extracted from the CFD simulations. The ".CGNS" files containing transient blade pressure at each time steps are also exported. In order to be able to average acoustic microphone pressure results in response, the transient source data is first split into blocks of 10 rotations each, resulting in 10 Hz frequency resolution. A 50 % overlap is chosen between the blocks which corresponds a total number of 12 blocks to be averaged. The same post-processing is used to all presented results using Hanning window and Amplitude Correction. The sound pressure level spectra of the blocks are finally RMS averaged.

Free-field

The acoustic results at the free-field microphones are computed for the three microphone positions located on an arch laying on the horizontal cut-plane of the fan as shown in Figure 2 (top left). The radius of the arch, hence the distance of the microphones to the rotation center, is equivalent to 10 fan tip radii. One microphone is located on the rotation axis downstream the fan, another on rotation plane and the third one upstream the fan with 30 degrees to the rotation axis.

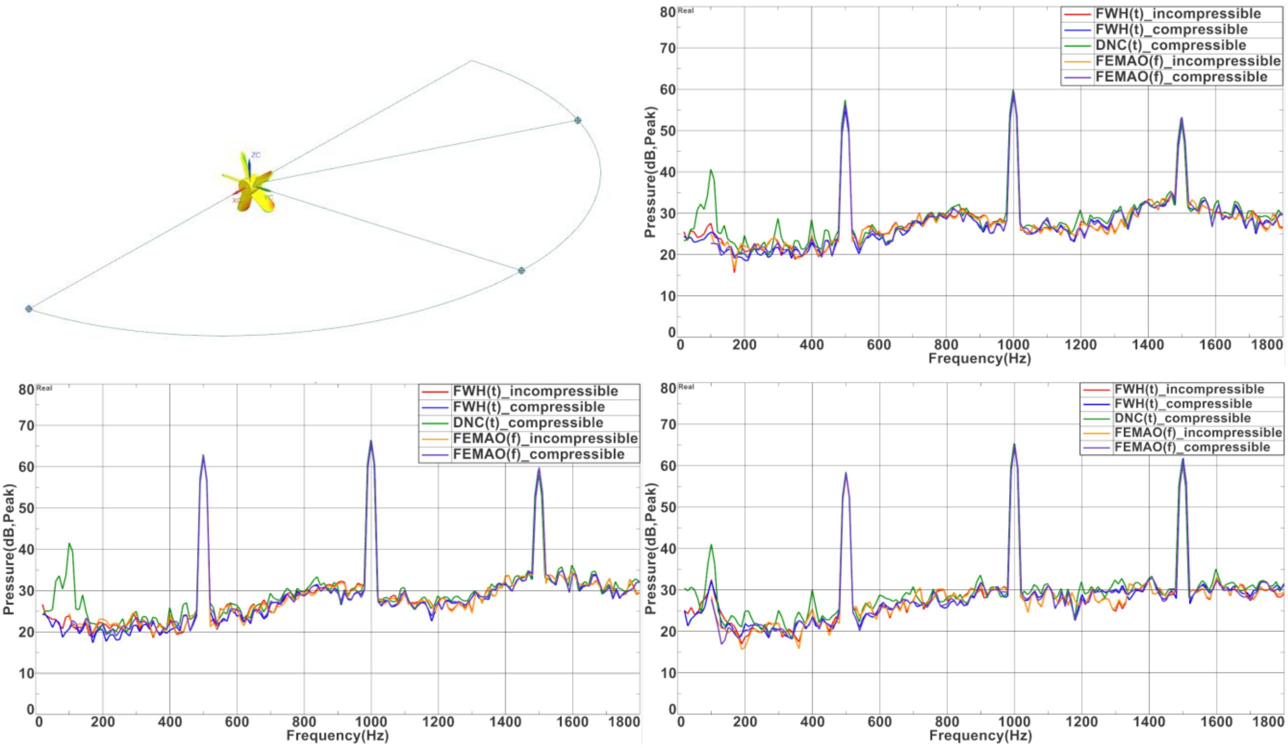

Figure 2: Free-field acoustic response with direct and hybrid solutions

All five free-field results at the far-field microphones are presented at Figure 2 for microphones on upstream the fan (top right), on rotation axis (bottom left), on rotation plane (bottom right). Red, blue, and green lines represent the time domain solutions as incompressible FW-H, compressible FW-H and DNC, respectively. The orange and purple lines represent the frequency domain solutions as incompressible input and compressible input, respectively. It can be seen that all five formulations provide the same sound pressure levels on the BPF and two higher harmonics for the tonal fan noise which is cross-validating the accuracy of the implementations and assumptions. Similarly, the broadband components also converge to the same sound pressure levels for all five curves for most of the frequencies of interest. Especially, all four hybrid solutions converge to the same levels within ± 2 dB while the DNC slightly deviates at lowest frequencies. This deviation might be due to the sponge layers in the DNC being too thin to suppress the lowest-frequency noise.

It is seen that the time and frequency domain hybrid techniques provide almost perfectly matching results once the input terms are consistent. Nevertheless, it is shown that, regardless of the selection of the acoustic analogy, similar free-field responses will be obtained in different simulations. For such anechoic-room like free-field fan noise applications in component level, indeed the hybrid solution can be found to be competitive to direct solution. However, one can add new microphone locations in the hybrid method easily and provide further insight into the acoustic directivity which will make it complementary to DNC, even in free-field, without re-running the CFD solution.

Contribution analysis to free-field response

For the frequency domain hybrid solution, the transient blade pressure is integrated over the compact blade segments to compute the source strength of the segment in time domain. In theory, a compact segment can be split into smaller compact segments and their total response should be equivalent to the one of the initial complete segment. In this exercise, as shown in Figure 3, the compact blade segments (left) are split in two compact segments representative of a leading edge one (center) and the trailing edge one (right), where the flow is from left to right.

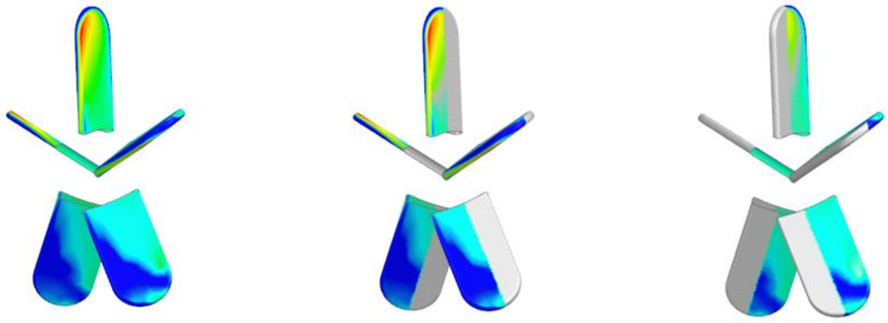

Figure 3: Contour plots representing blade segments for contribution analysis

In order to keep the segment centers of gravity constant in all applications for sake of comparison, the complete blade topology is considered in all three simulations. As shown as gray contours in Figure 3 (center), the leading edge segment loads are obtained by discarding the trailing edge segment contribution. Similarly, as represented in Figure 3 (right), the trailing edge source is obtained by discarding the leading edge one.

The contribution analysis is performed for the frequency domain hybrid approach with the incompressible flow solution over the same microphone locations as described above. Figure 4 shows the total response (solid red line) obtained with time domain hybrid solution with incompressible input. The leading edge and trailing edge segment contributions are shown with blue dashed and green dash-dot lines, respectively. As seen in all three microphone locations, the tonal noise at all BPFs is dominated by the leading edge component which can be expected due to the periodic blade interaction with the impinging jet stream. In this considered fan model and operating conditions, only the lowest frequencies of the broadband component are dominated by the leading edge segment. The sound pressure level at the broadband frequencies higher than the 1st BPF is found to be dominated by the trailing edge segment.

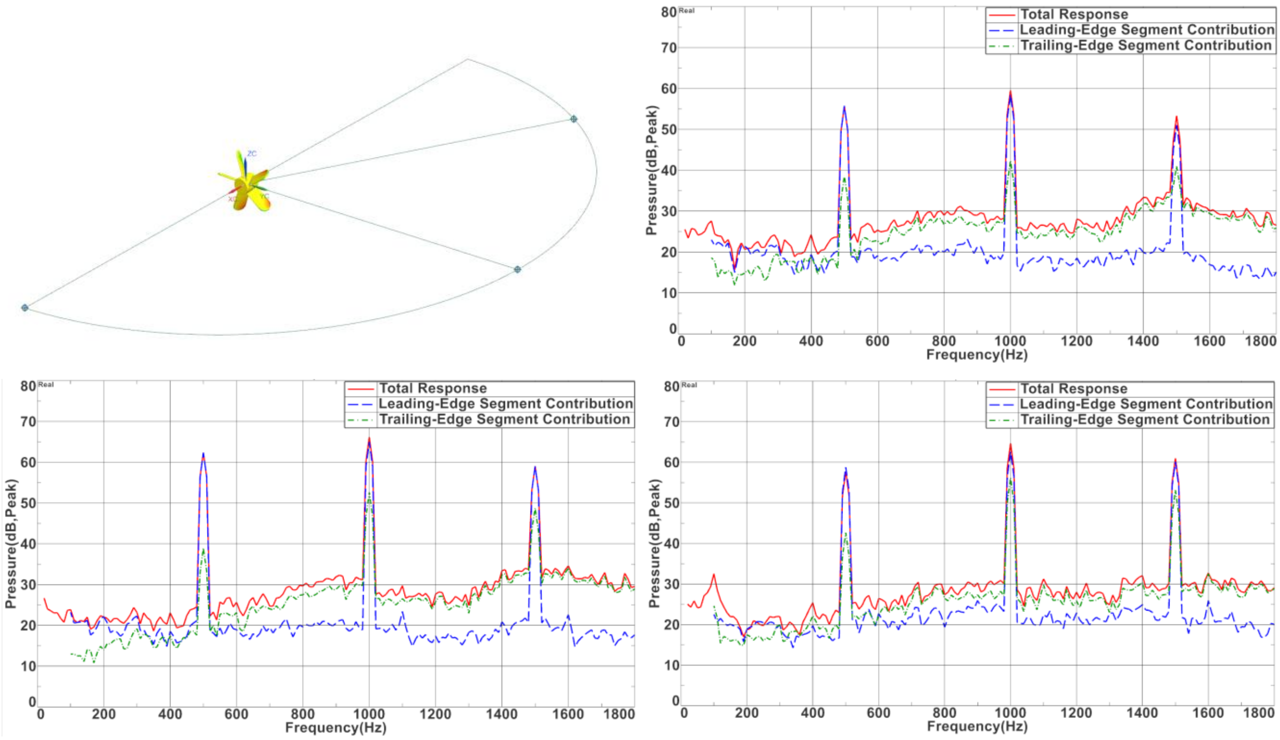

Figure 4: Free-field acoustic response with hybrid solutions with incompressible flow and contribution analysis

It is worth to remind that these results are obtained with RMS averaging of several blocks. In principle, there will be some cancellations between two segments which can be only accounted with the two segments used in the same solution. Nevertheless, this exercise provides further insight on which frequencies are dominated by which part of the blade segments. This is a complimentary capability of the hybrid solutions even in free-field, once again, without re-running the CFD simulation.

Installation effects

The most pronounced benefit of the frequency domain acoustic propagation is to be able to account for installation effects which might include reflective and absorbing boundaries or even porous media typical to realistic industrial problems. In order to demonstrate the effects of the surrounding surfaces in propagation, and in order to be able to validate with known analytical solutions [13], the virtual fan is assumed to be operated next to an infinitely large absorbing flat plate located 1.25 tip radius downstream, parallel to the fan rotation plane. It is worth to note that, for sake of comparison, the same CFD results are used both in absence and presence of the absorbing plane. Such a large and close surface is selected to amplify the effects of obstacles in acoustic propagation. Otherwise, for a more accurate interpretation, in such cases where the plate is located close to the fan, the CFD solution needs to be re-computed.

As shown in Figure 5, on top of the free-field fan (left), its geometrical image (center, light colored) is introduced 2.5 tip radii downstream the fan. The contour plots show the outcome of introducing the geometrical mirror of the fan on top of the free-field response. The real part of the acoustic pressure at the 1st BPF (500 Hz) is plotted at the microphones on a horizontal plane. The image fan appears to change the directivity of the propagation, keeping the phase distribution similar. This also forces a zero acoustic pressure on the mirror plane as seen in the contour plots.

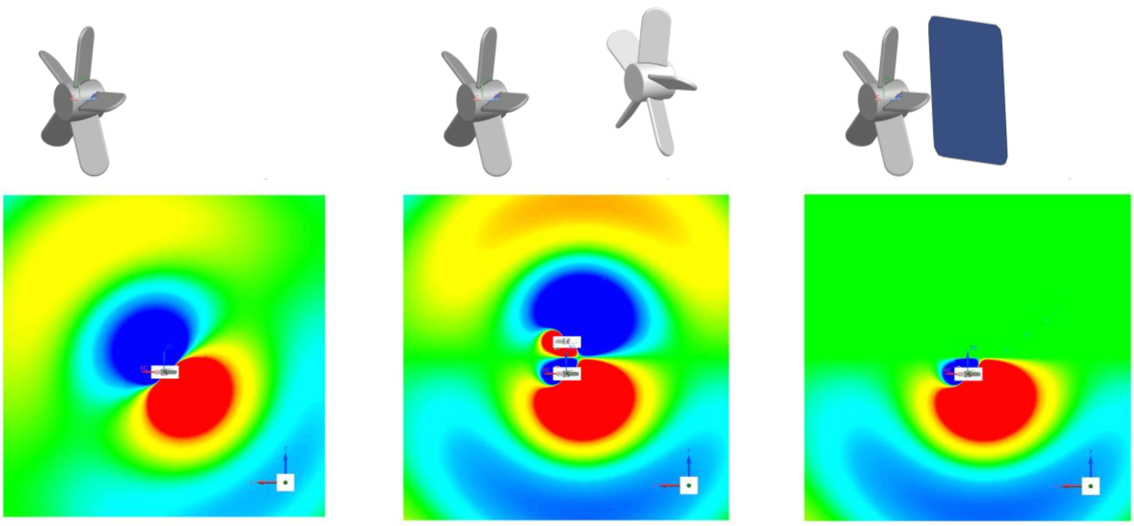

Figure 5: Free and scattered-field acoustic pressure contours in presence of rigid absorbing plane

In order to mimic the same behavior of the geometrically mirrored fan, one can create a small finite element domain with a very high admittance boundary condition applied on the flat surface as represented in Figure 5 (right top). The absorption condition at the exterior of the finite element domain due infinitely large plane is then provided by the so-called anti-symmetry (pressure release) boundary condition. It is an addition to the AML surface defined on the rest of the envelope faces as mentioned previously. Therefore, with these combinations, the envelope coinciding the flat plate of the finite element domain will serve as infinitely large absorbing plate. As shown in Figure 5 (right bottom), this combination will provide accurate results at microphones located both inside and outside of the finite element domain. As expected, there will be no acoustic pressure propagating outside of the absorbing surface. Even it is addressing a simple propagation problem, this exercise qualitatively validates the FEMAO methodology using fan source with installation effects which also includes absorbing surfaces.

The above exercise considers a scenario which results in changes in the directivity while keeping the dipole pattern in propagation. In presence of more complex geometries and reflective surface, the acoustic field can be dramatically changed. Another qualitative exercise is presented in Figure 6 for the 1st (top) and 2nd BPF (bottom) using the same incompressible CFD output files. The same fan now operates in presence of a fully rigid box which further modifies the propagated acoustic field. The internal and external acoustic fields of the box are separated with rigid boundaries while the transfer is only obtained by the openings of the circular fan and the rectangular grid, both located on the same face of the box. Even that the geometry is added on the plots, the scattering effects are first neglected, and the free-field contours are plotted in Figure 6 (left). Once the scattering effects of the rigid box are added (center), the amplitude and the directivity of the propagation changes significantly. The difference between free (thin red line) and installed (thick blue line) responses is also visible in the directivity plots (right). The microphones are located on the same plane as plotted in the contours and 2 wave-lengths away from the center of the rotation for the 1st BPF. Finally, for this geometry, the installation effects result in increase of the acoustic levels for the 1st BPF at all microphones on the directivity plane considered. Whereas for the 2nd BPF, the installed fan directivity results in lower acoustic levels for some of the microphones located at the other side of the box. This shows that the installation effects can amplify the sound pressure levels for some observers and mask for some others, depending on the frequency of interest and the geometry of choice. Nevertheless, since the used methodology is based on Finite Element framework in frequency domain, it can be used with arbitrary reflective and absorbing surface. This might let engineers to design their models where they can reduce noise levels for some expected observer locations by controlling the directivity of the propagation, especially once the source strength cannot be reduced.

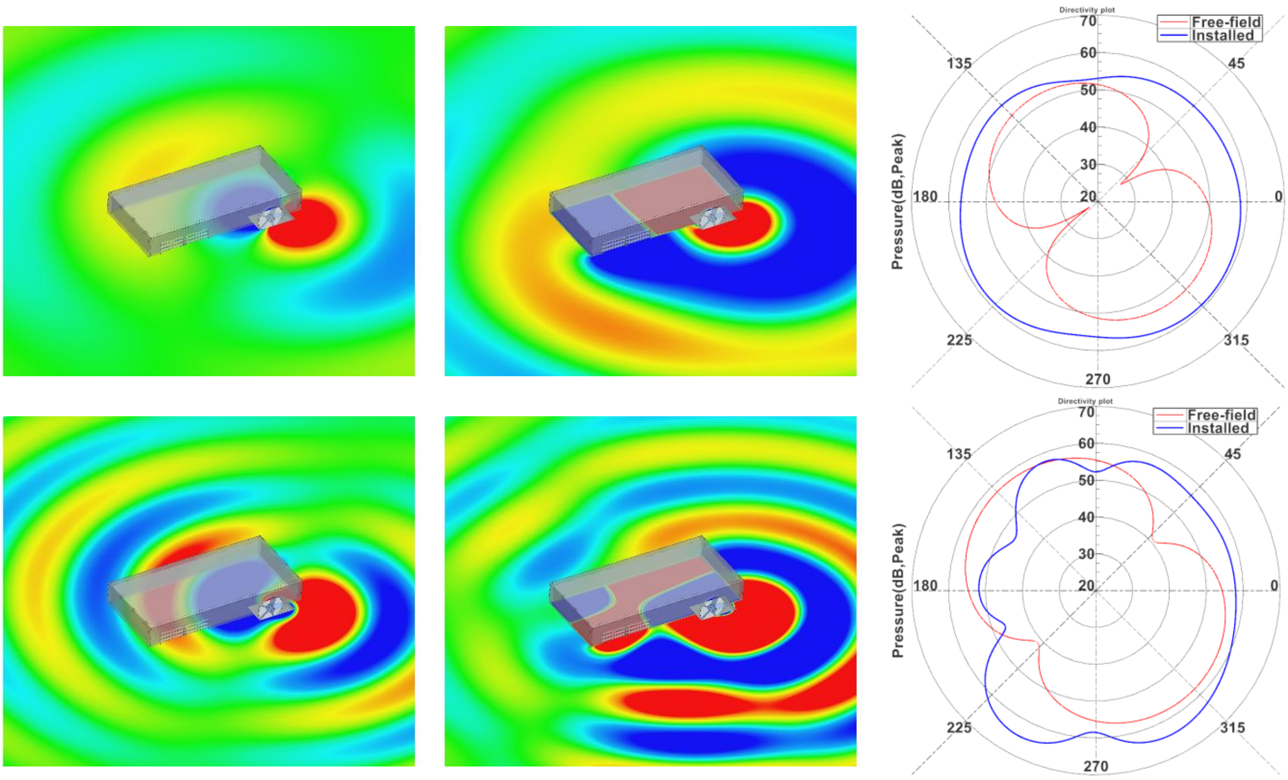

Figure 6: Free and scattered-field acoustic pressure contours of installed fan

CONCLUSION

Alternative aeroacoustics simulation methodologies are applied on a virtual low-speed axial fan. Using different techniques, varying from DNC to hybrid solutions coupled with time and frequency domain propagation, similar acoustic pressure levels are obtained in free-field. The cross-validation of various simulations highlights the accuracy of the hybrid methods. On top of its accuracy, a complementary benefit of the hybrid techniques is demonstrated by providing more insight via contribution analysis of dominant source segments without re-running the CFD solution. Last but not least, hybrid method is shown to complement the alternatives via accounting for reflection and absorption where the fan is installed, similar to the realistic applications.

ACKNOWLEDGEMENT

The authors thank Lars Erbig for the fruitful discussions regarding aeroacoustic analogies and his contribution to the paper.

BIBLIOGRAPHY

[1] A. Guédel, Y. Rozenberg, M. Roger, G. Perrin – *Prediction of fan trailing-edge noise*, Proceedings of Fan Noise 2007 Symposium, Lyon, **2007**

[2] J. Christophe, K. Kucukcoskun, D. Lallier-Daniels, M. Sanjose, S. Moreau – *Experimental Validation of Ducted Low-Speed Cooling Fan Noise Prediction Methods Including Broadband Scattering*, AIAA Aeroacoustics Conference, Lyon, **2016**

[3] T. Carolus, M. Schneider and H. Reese – *Axial flow broad-band noise and prediction*, Journal of Sound and Vibration, 300, **2007**

[4] D. von Werne, P. Chaduvula, P. Stahl, M. Jordan, et al. – *Fan Noise Prediction for Off-Highway Vehicle*, SAE Technical Paper 2017-01-1834, **2017**

[5] Simcenter STAR-CCM+ User Guide (version 2021.3)

[6] J. E. Ffowcs Williams, D. L. Hawkings – *Sound generation by turbulence and surfaces in arbitrary motion*, Phil. Trans. Roy. Soc., A264, **1969**

[7] F. Farassat – *Derivation of Formulations 1 and 1A of Farassat*, Technical Memorandum (NASA/TM-2007-214853), NASA Langley Research Center, **2007**

[8] M. Goldstein – *Aeroacoustics*, McGraw–Hill Inc., **1976**

[9] M. Roger – *Near-field fan noise modeling and installation effects due to scattering surfaces*, Proceedings of Fan Noise 2007 Symposium, Lyon, **2007**

[10] H. Beriot, A. Modave – *An automatic perfectly matched layer for acoustic finite element simulations in convex domains of general shape*, International Journal for Numerical Methods in Engineering, 122, **2021**

[11] H. Beriot, A. Prinn, G. Gabard – *Efficient implementation of high-order finite elements for Helmholtz problems*, International Journal for Numerical Methods in Engineering, 106, **2016**

[12] Simcenter Nastran Acoustics User's Guide (version 2022.1)

[13] A. Pierce – *Acoustics: An introduction to its physical principles and applications*, Ac. Soc. of America, **1989**